

**Electronic Supplementary Information (ESI)**

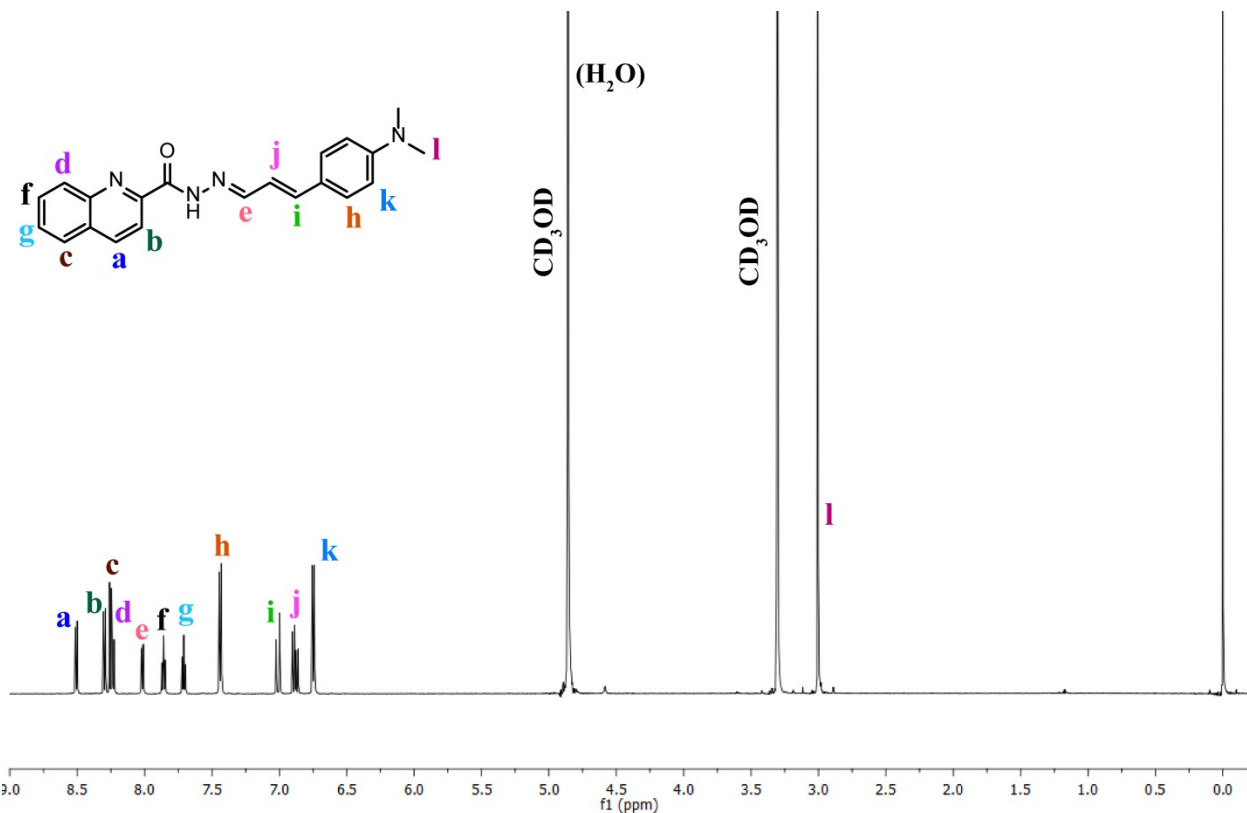
**Multi-responsive turn-on flurogenic probe to sense  $Zn^{2+}$ ,  
 $Cd^{2+}$  and  $Pb^{2+}$ : Left- Right-Center emission signal swing**

*Soham Samanta, Barun Kumar Datta, Madhurima Boral, Abhijit Nandan and  
Gopal Das\**

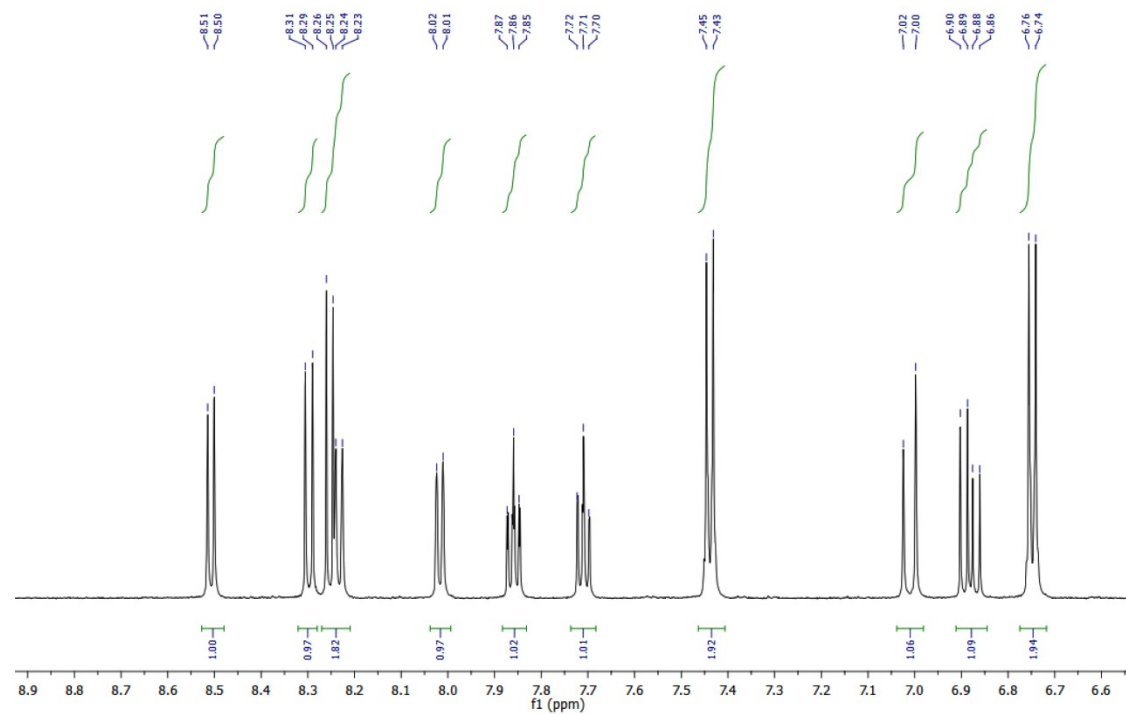
Department of Chemistry

Indian Institute of Technology Guwahati, Guwahati 781039, Assam, India

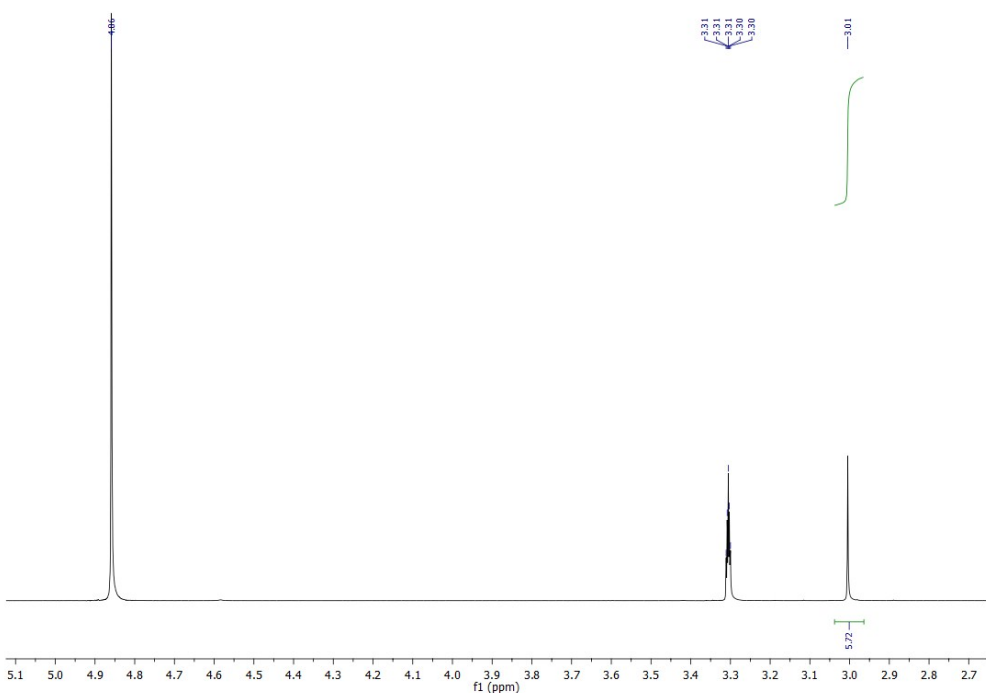
E-mail: gdas@iitg.ernet.in



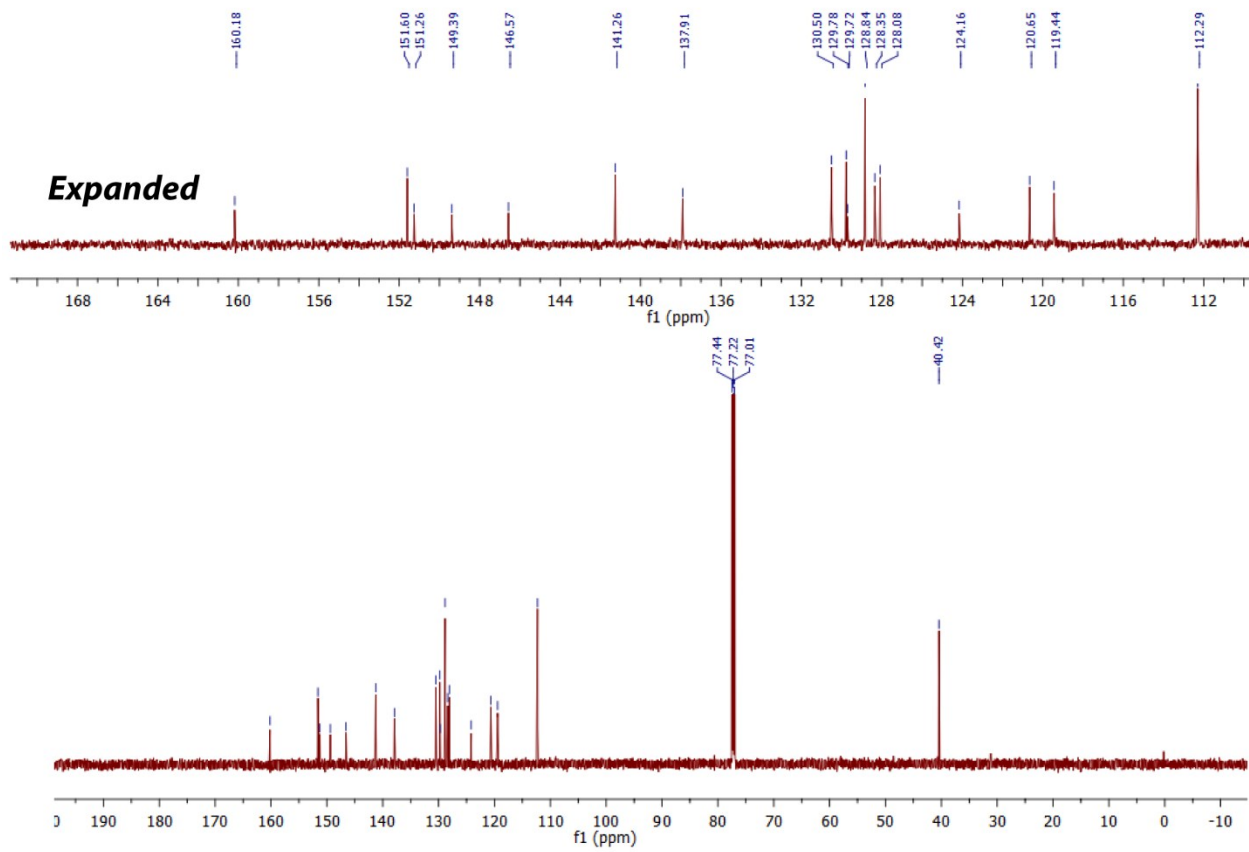
**Figure S1:**  $^1\text{H}$ -NMR spectra of **L**



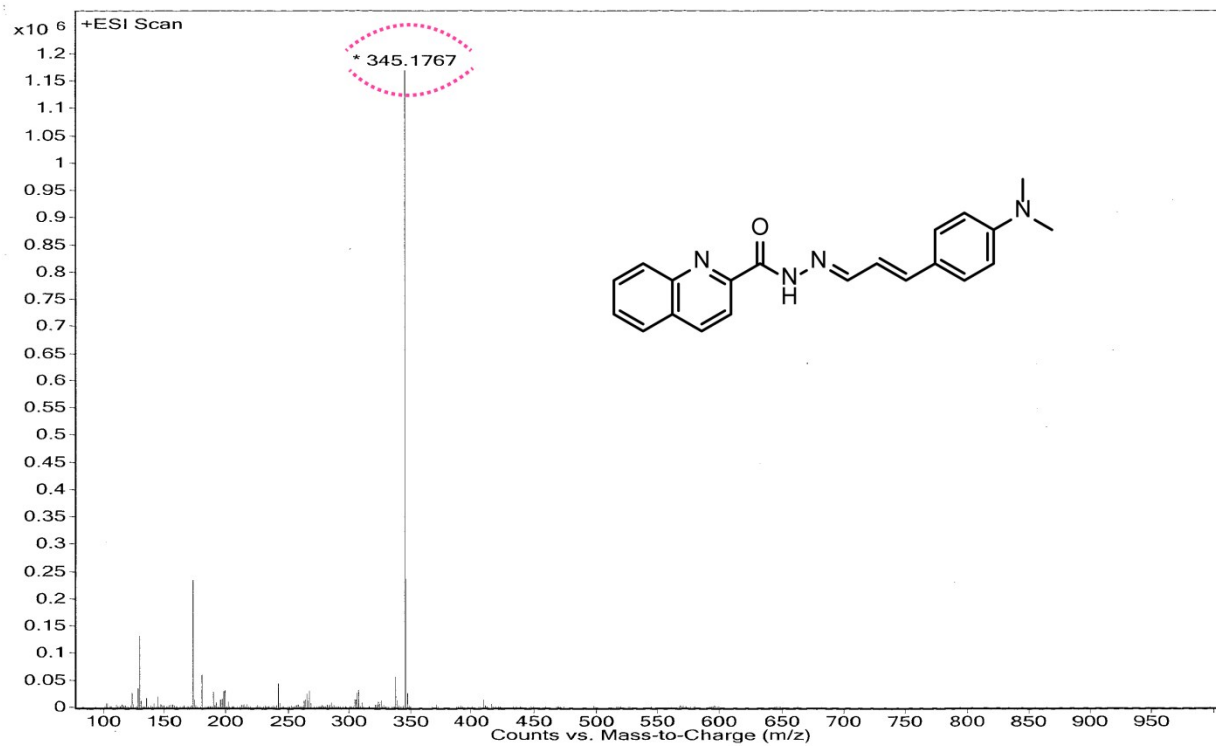
**Figure S2:** Expanded (aromatic region)  $^1\text{H}$ -NMR spectra of **L**



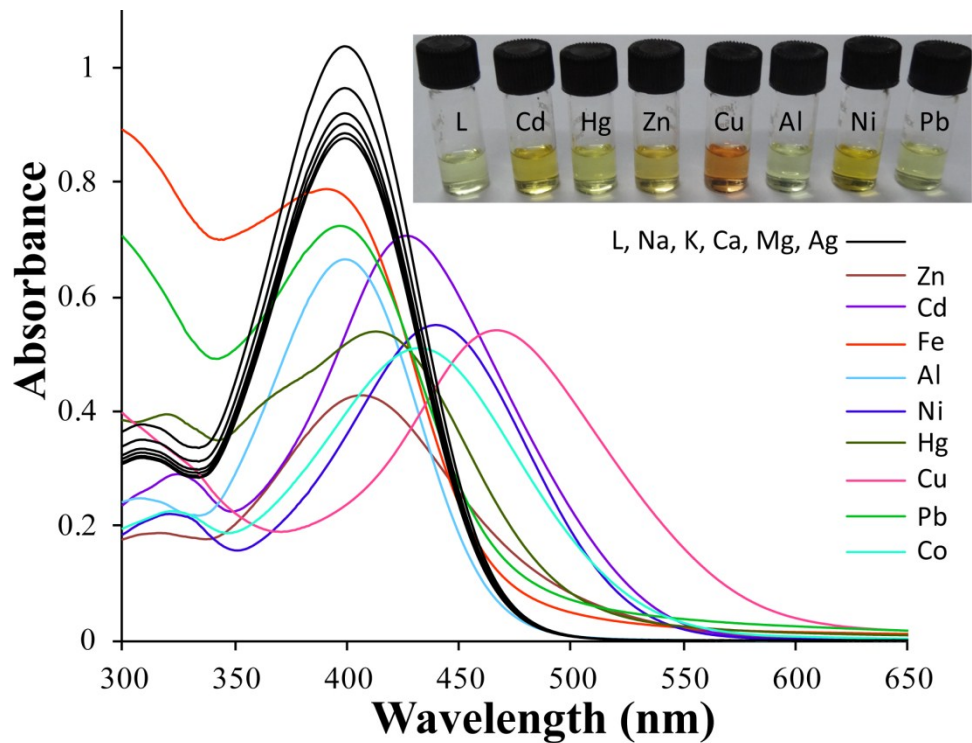
**Figure S3:** Expanded (aliphatic region)  $^1\text{H}$ -NMR spectra of **L**



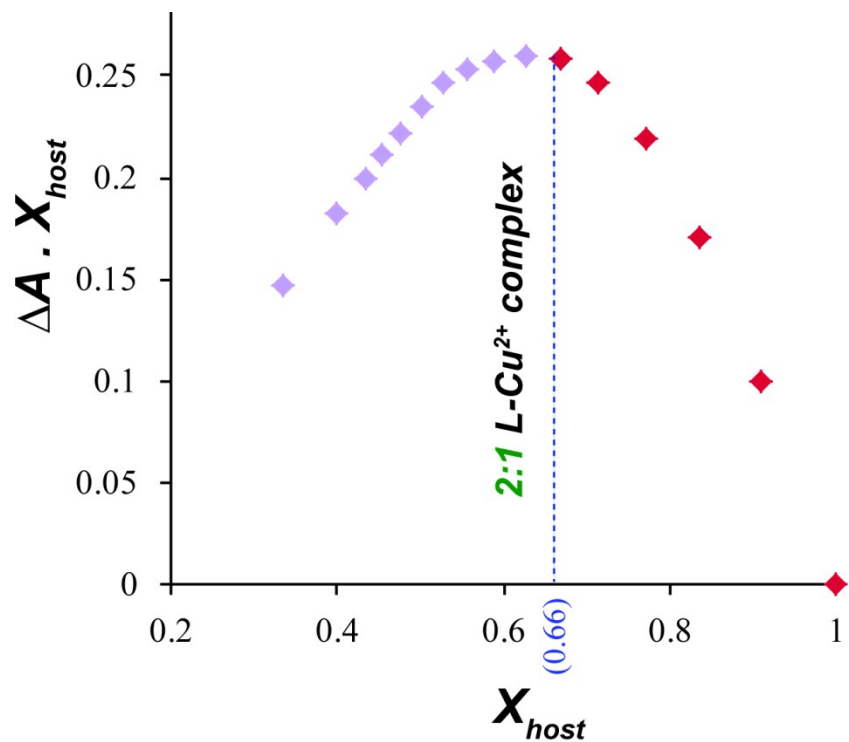
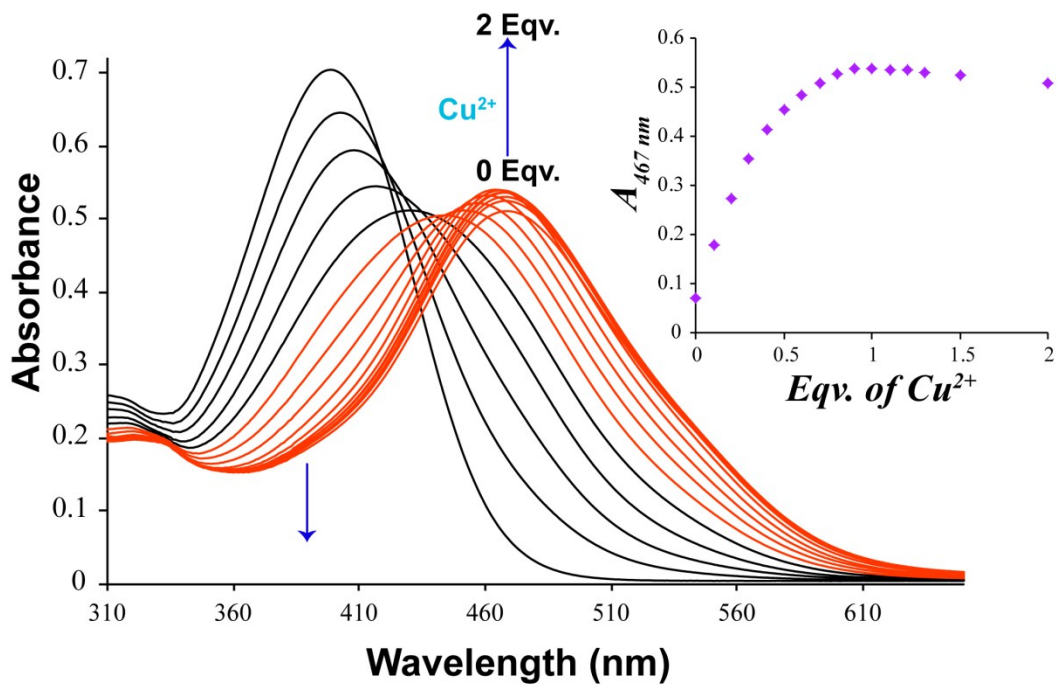
**Figure S4:**  $^{13}\text{C}$ -NMR spectra of **L**



**Figure S5:** Mass spectrum of **L**



**Figure S6:** UV-Vis spectra of **L** (10  $\mu$ M) in presence of excess (20 equivalents) of various metal ions in  $\text{CH}_3\text{OH}$ /aqueous HEPES buffer (5 mM, pH~7.3; 4:1, v/v) mixed solvent



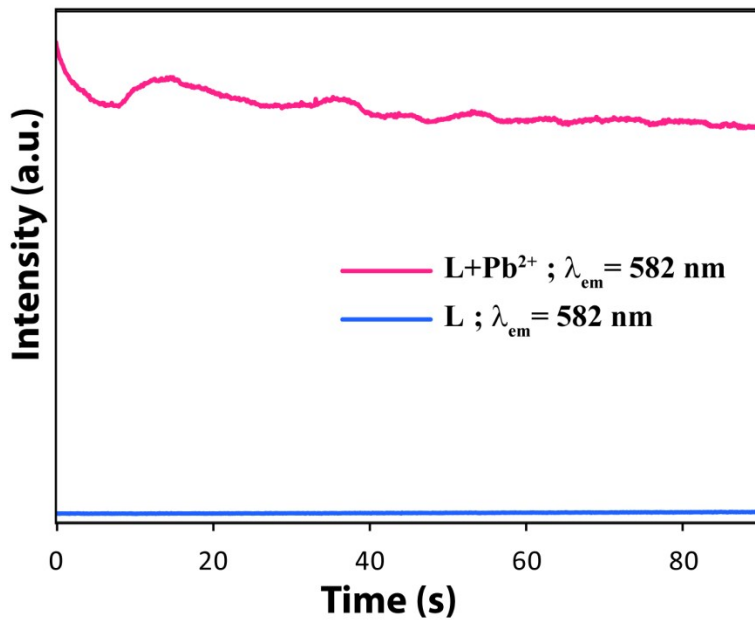


**Figure S9:** Changes in the emission intensity of L at 582 nm with time upon interaction with Pb<sup>2+</sup>;  $\lambda_{\text{ex}} = 450 \text{ nm}$

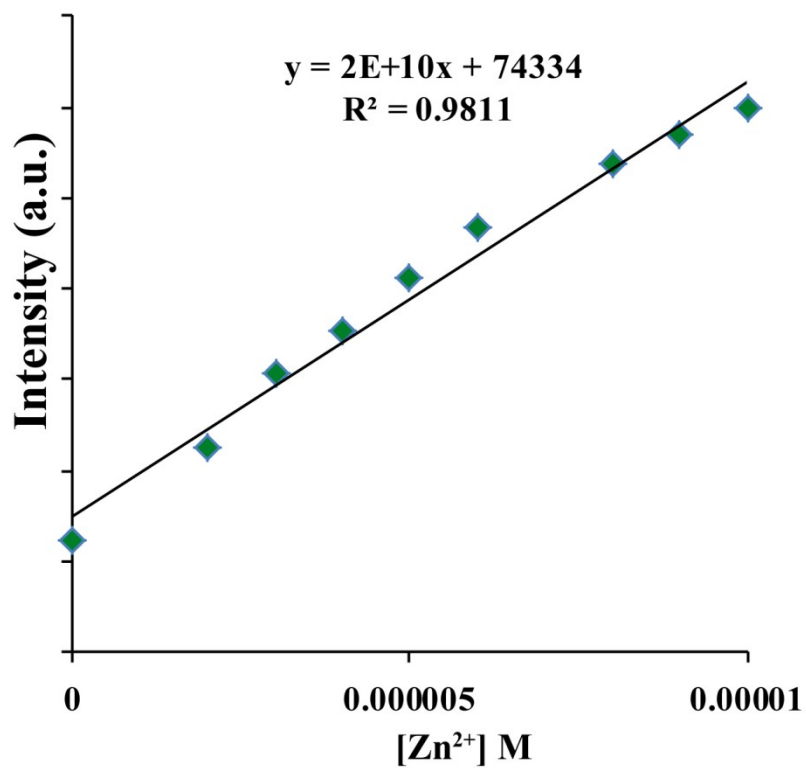


**Figure S10:** Fluorescence intensity vs. concentration of Zn<sup>2+</sup> plot for determination of detection limit

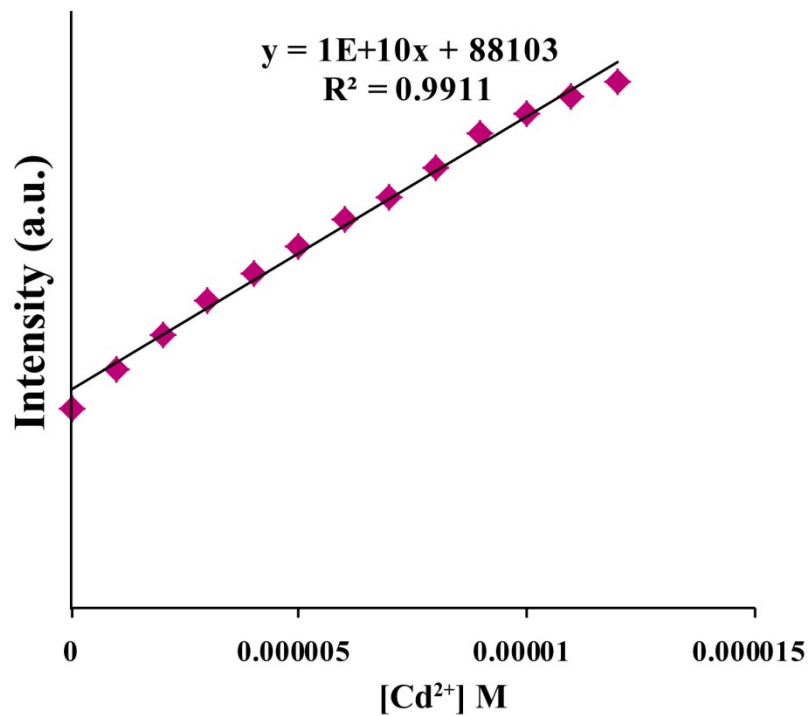


**Figure S11:** Fluorescence intensity vs. concentration of  $\text{Cd}^{2+}$  plot for determination of detection limit

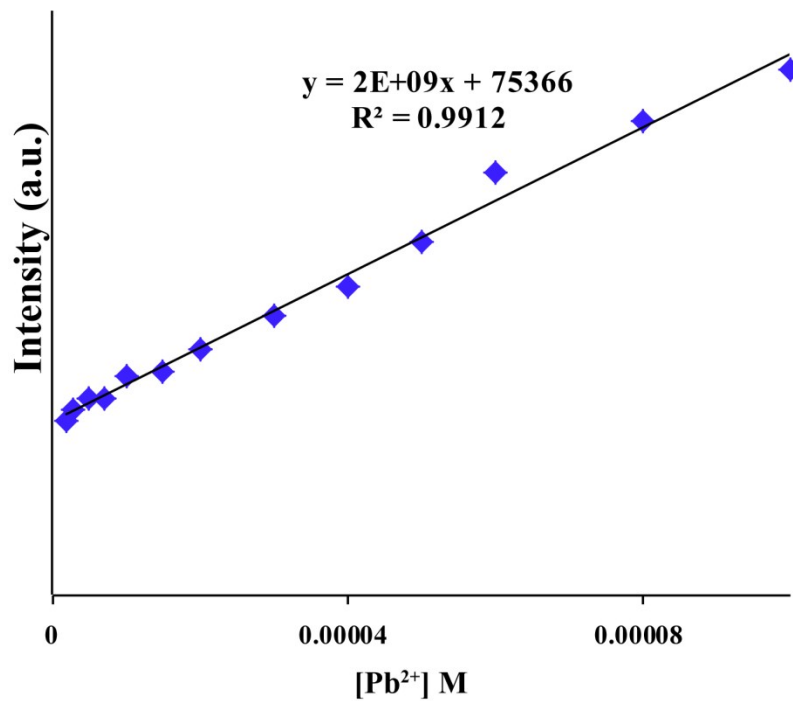


**Figure S12:** Fluorescence intensity vs. concentration of  $\text{Pb}^{2+}$  plot for determination of detection limit

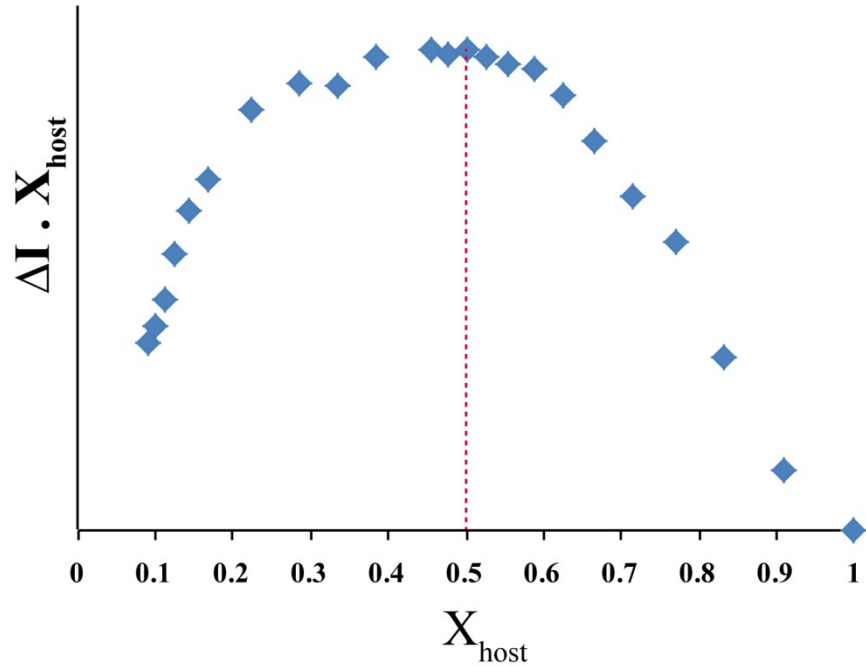


**Figure S13:** Job's plot for  $\text{Zn}^{2+}$  from the fluorescence titration spectra

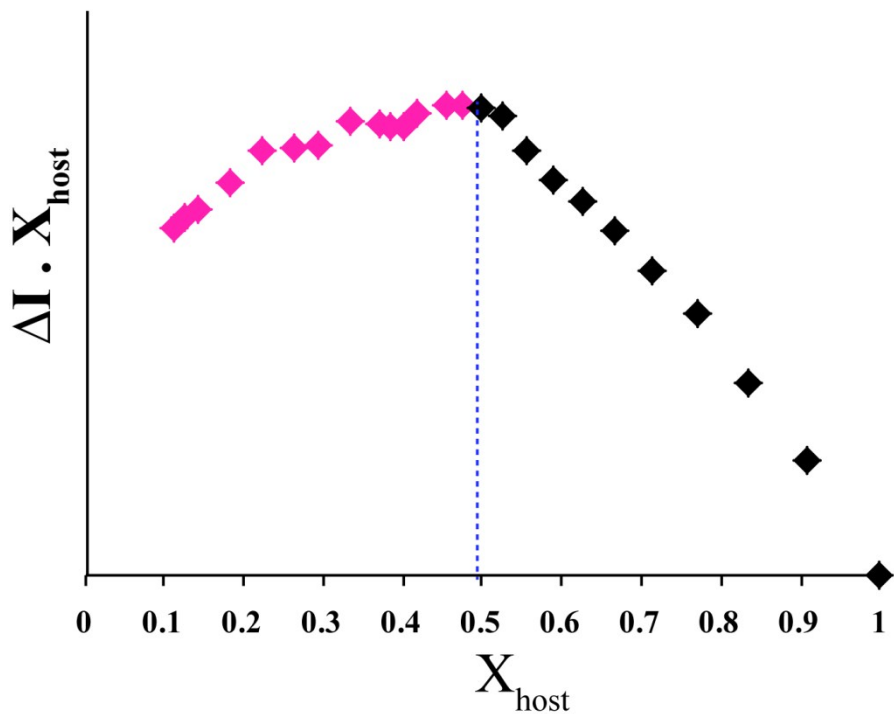


**Figure S14:** Job's plot for  $\text{Cd}^{2+}$  from the fluorescence titration spectra

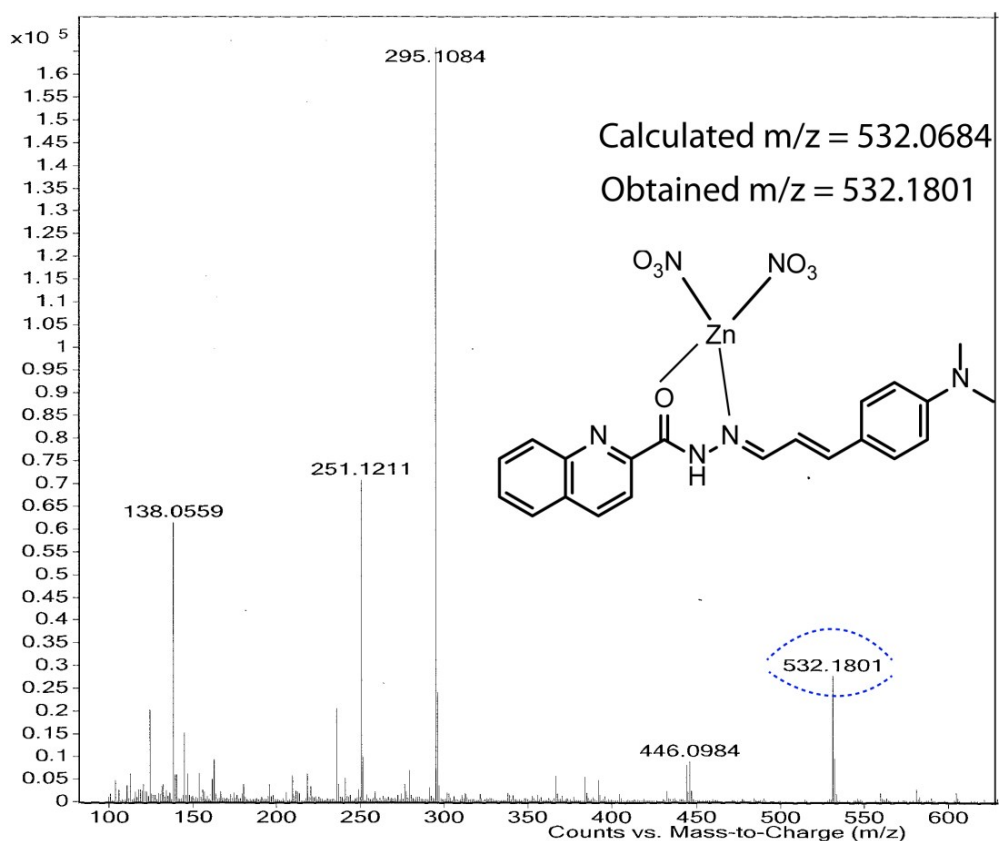


**Figure S15.** Mass spectrum of L in presence of  $Zn^{2+}$

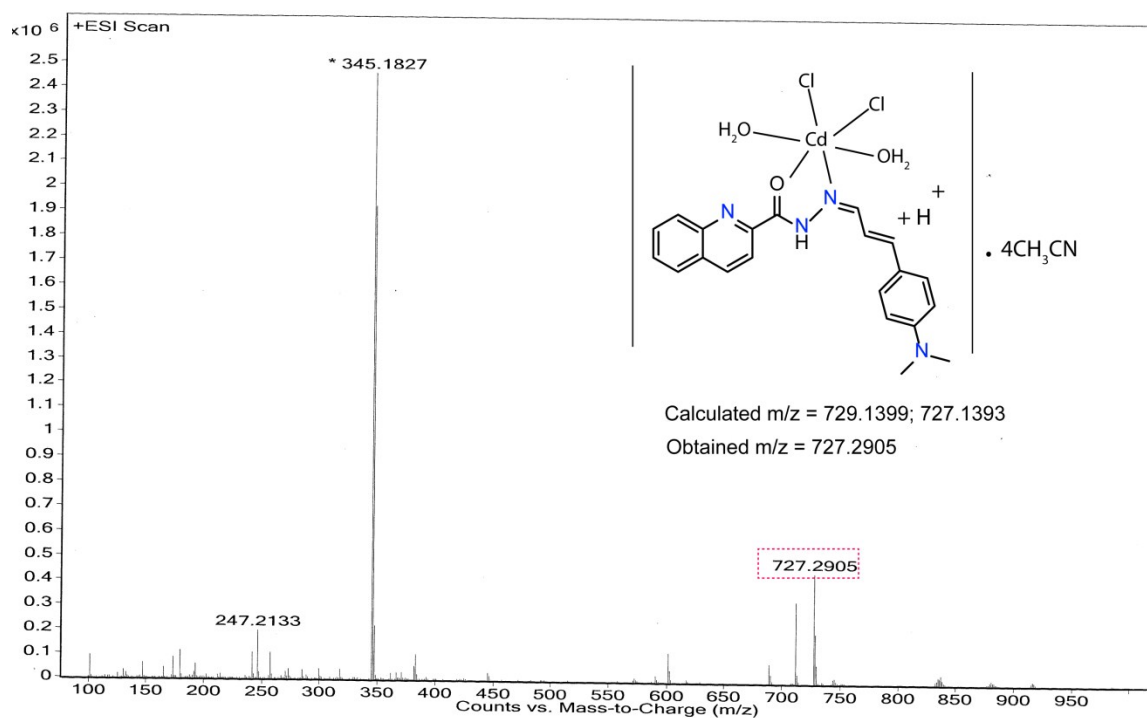


**Figure S16.** Mass spectrum of L in presence of  $Cd^{2+}$

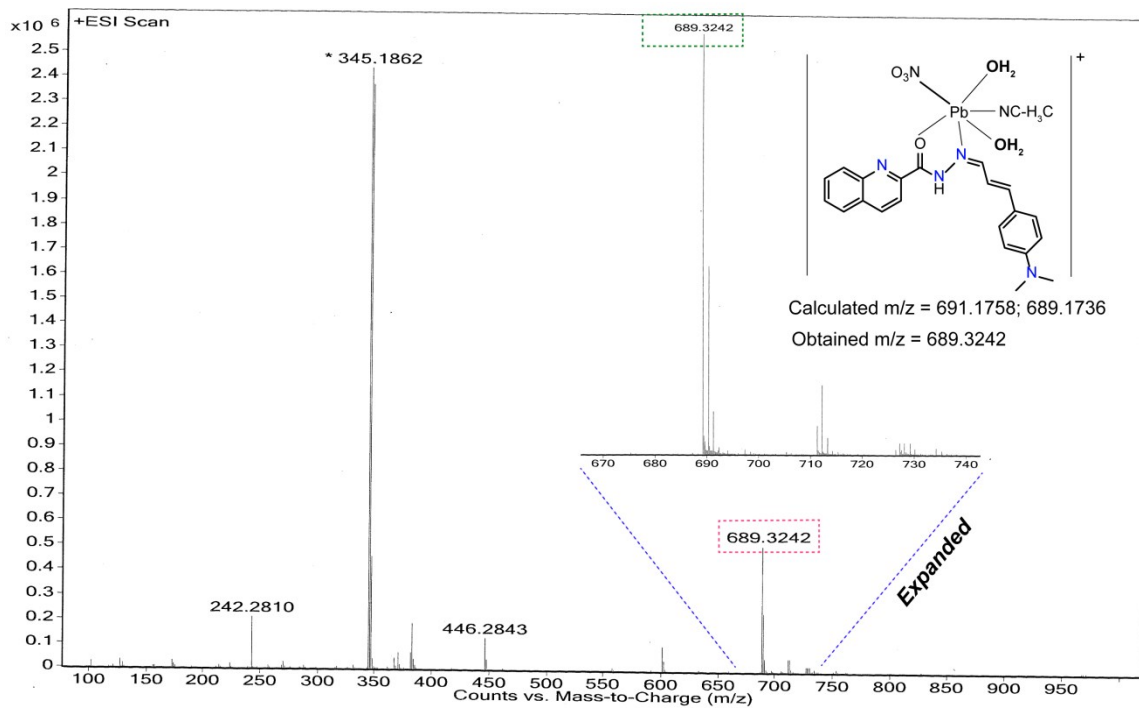


**Figure S17:** Mass spectrum of **L** in presence of  $\text{Pb}^{2+}$

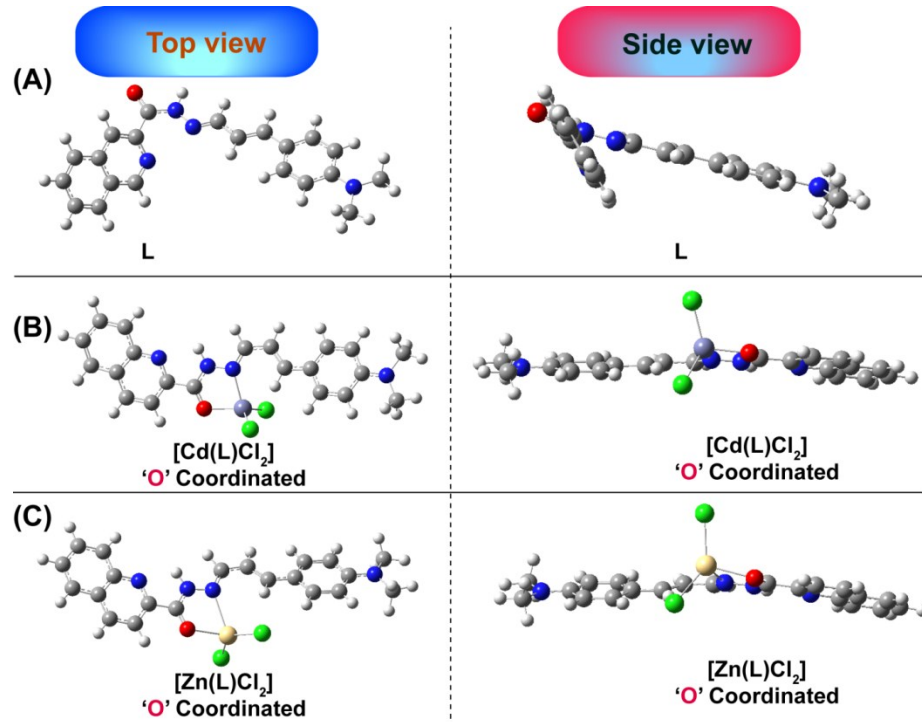


**Figure S18:** Optimized structures of **L** and its  $\text{Cd}^{2+}$  and  $\text{Zn}^{2+}$  complexes. For **L** and it's  $\text{Zn}^{2+}$  complex the calculations were performed using B3LYP/6-31 G (d,p) as implemented on Gaussian 09. For **L-Cd<sup>2+</sup>** complex calculation was performed using B3LYP/6-31 G (d) basis set for all the atoms except for  $\text{Cd}^{2+}$ , where LANL2DZ effective core potential (ECP) was employed.

**References:**

1. M. J. Frisch, G. W. Trucks, H. B. Schlegel, G. E. Scuseria, M. A. Robb, J. R. Cheeseman, G. Scalmani, V. Barone, B. Mennucci, G. A. Petersson, H. Nakatsuji, M. Caricato, X. Li, H. P. Hratchian, A. F. Izmaylov, J. Bloino, G. Zheng, J. L. Sonnenberg, M. Hada, M. Ehara, K. Toyota, R. Fukuda, J. Hasegawa, M. Ishida, T. Nakajima, Y. Honda, O. Kitao, H. Nakai, T. Vreven, J. A. Montgomery, Jr., J. E. Peralta, F. Ogliaro, M. Bearpark, J. J. Heyd, E. Brothers, K. N. Kudin, V. N. Staroverov, T. Keith, R. Kobayashi, J. Normand, K. Raghavachari, A. Rendell, J. C. Burant, S. S. Iyengar, J. Tomasi, M. Cossi, N. Rega, J. M. Millam, M. Klene, J. E. Knox, J. B. Cross, V. Bakken, C. Adamo, J. Jaramillo, R. Gomperts, R. E. Stratmann, O. Yazyev, A. J. Austin, R. Cammi, C. Pomelli, J. W. Ochterski, R. L. Martin, K. Morokuma, V. G. Zakrzewski, G. A. Voth, P. Salvador, J. J. Dannenberg, S. Dapprich, A. D. Daniels, O. Farkas, J. B. Foresman, J. V. Ortiz, J. Cioslowski, and D. J. Fox, *Gaussian 09, Revision D.01*, Gaussian, Inc., Wallingford CT, 2013.